

Wavefunction-Engineering of the Optoelectronic Yield for Intersubband THz-Laser Nanodevices

E. A. ANAGNOSTAKIS

Nanodevice Physics Forum; Athens, Greece.
22 Kalamakiou Ave., GR 174 55 Alimos, Greece.
emmanagn@otenet.gr

Abstract

A novel THz-luminescence LASER nanoheterostructure of the intersubband, longer-wavelength limit, mid-infrared functionality type is designed on the basis of optically pumped dual resonant tunnelling of conductivity electrons within an appropriately energetically determined scheme of five subbands hosted by two communicating asymmetric approximately rectangular quantum wells (QWs).

The upper LASER action level employed is the second excited subband of the nanostructure back, wider QW and is being provided with electrons via resonant tunnelling from the first excited subband of the nanostructure front QW being populated through remotely ignited optical pumping out of the local fundamental subband.

As the lower LASER action level, on the other hand, functions the first excited back QW subband, directly delivering the received electrons to the local fundamental subband – via a fast vertical longitudinal optical phonon scattering-, wherefrom they are being recycled back to the nanostructure front QW fundamental subband by virtue of a second – reverse sense – resonant tunnelling – mediated normal charge transport mechanism.

LASER action level population inversion and intersubband transition (ISBT) effective dipole lengths are critically monitored in connexion to the pertinent ISBT oscillator strengths and device stimulated optical gain achievable.

I. Introduction

The investigation of semiconductor heterointerfaces is a prominent subject of ongoing research in view of the crucial importance which they possess for the functionality of numerous optoelectronic microdevices [1 – 6].

For more than two decades, the designing strategy of wavefunction-engineering [7] has systematically been giving birth to an admirable wealth of innovative

semiconductor devices offering a high degree of tunability in their optoelectronic performance.

Celebrated pioneering microelectronic heterostructures of the kind have been the Bloch oscillator [8, 9], the resonant tunnelling double heterodiode [10], the hot electron tunnelling transistor [11], and the revolutionary quantum cascade LASER [12, 13].

In the present Paper, the principle of operation of an intersubband, far mid-infrared

unipolar LASER action heterostructure based on optically pumped dual resonant tunnelling between two both spatially and energetic depth – wise asymmetric quantum wells (QWs) is outlined in terms of band gap engineering and quantum mechanical conductivity electron vertical transport and local energetic transition functionality.

The required LASER action level population inversion is monitored via a rate equation formalism against the ratio of the crucial time constants characterising the two successive resonant tunnelling processes involved along with the intervening intersubband longitudinal optical phonon scattering. A generic application of the operational principle to a model four-semiconductor nanostructure predictably emitting in the 20 μm far mid – infrared coherent electromagnetic radiation spectrum band is discussed, with a measure of the designed nanodevice optoelectronic yield given by the intersubband stimulated optical gain, expressible through the LASER action population inversion in terms of the subband lifetimes entailed.

Wavefunction-Engineering

The present Paper aims at proposing a novel LASER action nanoheterostructure [14] operational principle based on remotely optically pumped [15, 16] dual resonant tunnelling (OPRT) unipolar charge transport mechanism materialisable within the framework of two communicating quantum wells (CQWs), asymmetric *both* in the their spatial extension *and* energetic barrier height aspect, hosting a total of five partially localised subbands – two (the fundamental $\text{If}^>$ and first excited $\text{If}^{'>}$) on the part of the envisaged device front [F] QW and the remaining three (the fundamental $\text{Ib}^>$, the first excited $\text{Ib}^{'>}$, and the second excited $\text{Ib}^{''>}$) on the other part, of the OPRT device back [B] QW-, a band gap engineering designing meant to have established two selective, achievable by a nanostructure respective growth procedure, energy matchings; one between the uppermost subbands $\text{If}^{'>}$ and $\text{Ib}^{''>}$ of the two CQWs and another concerning the two neighbouring QWs innermost fundamental sublevels $\text{If}^>$ and $\text{Ib}^>$ (Figure 1).

II. Proposed THz-LASER Yield

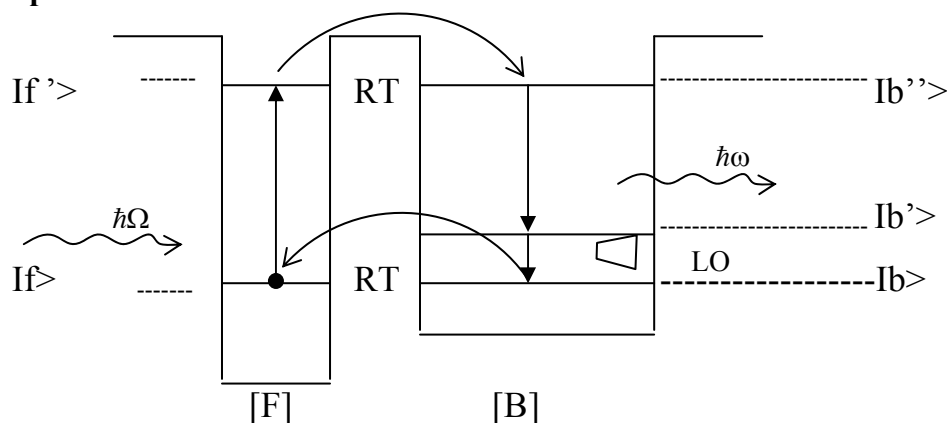


Figure 1. Wavefunction-engineering of the proposed THz-LASER.

The two LASER action OPRT nanodevice levels are designed to be the second excited $Ib''>$ back [B] QW subband and the local next lower first excited $Ib'>$ one:

The upper OPRT LASER action level is predicted to be being provided with conductivity electrons resonantly tunnelling [17, 18] into it out of its energetically matched device front [F] QW first excited $If'>$ subband, being populated through remotely ignited optical intersubband pumping from its local fundamental $If>$, front QW, subband. The lower OPRT nanostructure LASER action level is, on the other hand, expected to be directly delivering its radiatively de – excited electrons to the local, device back [B] QW, fundamental $Ib>$ subband via a particularly fast longitudinal optical (LO) phonon scattering, almost vertical in the reciprocal space, favoured by a band gap – engineered energetic proximity of the entailed

$Ib'> \leftrightarrow Ib>$ intersubband separation with the characteristic LO phonon energy valid under the device operational conditions entailed within the [B] QW semiconductor material.

The considered OPRT LASER nanostructure resonant microcavity functionality [19, 21] is, furthermore, determined by the above LO phonon scattering of radiatively down – converted conductivity electrons (from the LASER action lower level to the local [B] QW fundamental subband) being succeeded by their being recycled back to the OPRT LASER nanostructure [F] QW fundamental $If>$ subband by virtue of a second – reverse sense – resonant tunnelling – mediated normal charge transport mechanism.

The rate equation modelling of the LASER action functionality of subband levels $Ib''>$ and $Ib'>$ is taken of the form:

$$\frac{dN_{Ib''>}}{dt} = \frac{1}{T_{FB}} N_{If'>} - \frac{1}{\tau_{Ib''>}} N_{Ib''>} \quad (1),$$

$$\frac{dN_{Ib'>}}{dt} = \frac{1}{\tau} N_{Ib''>} - \frac{1}{\tau_{Ib'>}} N_{Ib'>} \quad (2),$$

with $N_{If'>}$, $N_{Ib'>}$ and $N_{Ib''>}$ being the sheet electron concentration of nanostructure resonator level $If'>$, $Ib'>$ and $Ib''>$, respectively, $\frac{1}{T_{FB}}$ being the temporal rate of achieving the resonant tunnelling charge transport from the [F] QW first excited subband $If'>$ onto the energetically commensurate [B] QW second

excited subband $Ib''>$, $\tau_{Ib''>}$ being the total lifetime of upper LASER action level $Ib''>$ - expressible by means of the combined radiative and non-radiative $Ib''> \rightarrow Ib>$ down – conversion rate $\frac{1}{\tau}$ and the non – radiative direct $Ib''> \rightarrow Ib>$ relaxation rate $\frac{1}{\tau_{Ib''> \rightarrow Ib>}}$ as

$$\frac{1}{\tau_{Ib''>}} = \frac{1}{\tau} + \frac{1}{\tau_{Ib''> \rightarrow Ib>}} \quad (3),$$

and $\frac{1}{\tau_{Ib'>}}$ being the non – radiative, fast vertical longitudinal optical phonon scattering rate of electrons received by the lower LASER action subband $Ib'>$ to the

local, [B] QW, fundamental subband $Ib>$.

(1) and (2) form a system in five unknowns, namely $N_{Ic>}$ ($c = f, f', b, b', b''$) – the areal electron densities of the five nanostructure resonator levels $Ic>$ -, along with the following equations:

$$\frac{dN_{If>}}{dt} = \frac{1}{T_{BF}} N_{Ib>} - \frac{I\Sigma}{\hbar\Omega} N_{If>} \quad (4),$$

$$\frac{dN_{If'>}}{dt} = \frac{I\Sigma}{\hbar\Omega} N_{If>} - \frac{1}{T_{FB}} N_{If'>} \quad (5),$$

$$\frac{dN_{Ib>}}{dt} = \frac{1}{\tau_{Ib''> \rightarrow Ib>}} N_{Ib''>} + \frac{1}{\tau_{Ib'>}} N_{Ib'>} - \frac{1}{T_{BF}} N_{Ib>} \quad (6),$$

where $\frac{1}{T_{BF}}$ denotes the temporal rate at which the (reverse sense) $Ib> \rightarrow If>$ resonant electron tunnelling is effected within the CQWs, I the optical pumping intensity, Ω the pumping photon cyclic frequency, and Σ the optical absorption cross

section exhibited by electrons initially resting upon [F] QW fundamental subband level $If>$ to incoming pumping photons.

On the other hand, the quantum mechanically thus designed stimulated optical yield Y is determined as [15]

$$Y = \frac{1}{L} \sigma \Delta N \quad (7),$$

with L being the spatial extension of the entire CQWs configuration, σ the LASER stimulated emission cross section, for producing the secondary, coherent photons (of energy $\hbar\omega = \Delta E_{Ib''> \rightarrow Ib'>} = \Delta E$), and ΔN the LASER action population inversion between levels $Ib''>$ and $Ib'>$ obtained from the above electron concentration rate equation system solved at the steady state of the concurrency of the different charge

transport mechanisms within the OPRT nanoheterostructure.

The aforementioned model formalism employed – based upon the rate equation monitoring of the proposed OPRT LASER action level population evolution and inversion – incorporates the transmission coefficient determination [14, 17] for the resonant tunnelling inter – QW communication mechanism consecutive steps.

III. Model Application of the Proposed OPRT LASER

For studying the applicability of the herewith proposed optically pumped dual resonant tunnelling LASER action unipolar charge transport mechanism we now consider an indicative generic semiconductor nanoheterostructure based on the conventional $\text{Al}_x\text{Ga}_{1-x}\text{As}/\text{GaAs}$ material system.

In particular, we employ two totally asymmetric – both in the spatial width and in the energetic barrier height –, communicating through an intervening barrier layer, approximately rectangular quantum wells, both formulated within (different portions of) the GaAs semiconductor: The front QW [F] of spatial width 96 \AA and energetic barrier height 221 meV , contained between a surface $\text{Al}_{0.3}\text{Ga}_{0.7}\text{As}$ slab and the inter – QW communication barrier layer, and the back QW [B] of growth axis extension 162 \AA and energetic confinement hill 204 meV , spanning the region between the inter – QW communication barrier layer and a bottom $\text{Al}_{0.33}\text{Ga}_{0.67}\text{As}$ slab. The intervening, inter – QW communication barrier layer may non – exclusively be regarded as the succession (either abrupt or graded) of two rather equithick sublayers of $\text{Al}_{0.3}\text{Ga}_{0.7}\text{As}$ and $\text{Al}_{0.33}\text{Ga}_{0.67}\text{As}$.

The major goal attempted by the above employment is the establishment of a specific band gap engineering depicting the desired novelty of *double* (both spatial and energetic trench – wice) asymmetry between the two successive

Functionality and Yield Designing to a Generic Nanostructure and Discussion

communicating QWs embodying the crucial nanostructure hosting the prescheduled five in all conduction subbands fulfilling the dual energy matching (both between the uppermost energy levels of the two QWs and between the lowest two, fundamental, subbands of theirs) needed for the possibility of the (optically ignited) dual resonant tunnelling inter – QW communication.

For the computational technique utilised for self – consistently depicting the energy eigenvalues above, the Sturm – Liouville eigenvalue problem comprising the quantum mechanical Schroedinger differential equation and the appropriate exact boundary conditions conjugate with the entailed eigenfunction vanishing asymptotically at infinities is treated by the finite difference method after the employment of an independent variable transformation restricting the integration domain to the finite, universal, dimensionless interval $[-1, 1]$. The handling of the problem evolves into the numerical calculation of the eigenvectors and respective eigenvalues of a specific tridiagonal matrix hosting the three successions of coefficients appearing in the kind of finite difference equations selected to convergently approach the initial Sturm – Liouville differential equation [22].

With respect to the generic situation of a conductivity electron being hosted by the quantum well (QW) of potential energy profile $U(x)$ against the growth axis coordinate x within a conventional semiconductor nanodevice heterointerface, the pertinent Schrödinger equation, concerning the electron de Broglie time – independent wavefunction $\psi(x)$ and taking into account the spatial variation $m^*(x)$ of the carrier effective mass, reads:

$$-\frac{d}{dx} \left[\frac{\hbar^2}{2m^*(x)} \frac{d\psi(x)}{dx} \right] + U(x) \psi(x) = E \psi(x), \quad (8)$$

with E being the allowed energy eigenvalue conjugate to each physically meaningful wavefunction $\psi(x)$, solving (8) and vanishing asymptotically at infinities,

and \hbar being Planck's action constant divided by 2π .

Performing, now, an independent variable transformation, namely,

$$\chi \equiv \alpha x^* \operatorname{Arctanh}(\xi) \leftrightarrow \varphi(\xi) \equiv \psi[x(\xi)], \quad (9)$$

we obtain in place of (8) the Sturm – Liouville differential equation

$$\frac{d}{d\xi} \left[\mu(\xi) \frac{d\varphi(\xi)}{d\xi} \right] - \nu(\xi) \varphi(\xi) + \lambda \sigma(\xi) \varphi(\xi) = 0, \quad (10)$$

under the boundary conditions

$$\varphi(-1) = 0 \text{ \& } \varphi(+1) = 0, \quad (11)$$

with functions $\mu(\xi)$, $\nu(\xi)$ and $\sigma(\xi)$ in the new dimensionless variable ξ

(belonging to the universal interval $[-1, +1]$) defined as

$$\mu(\xi) \equiv \frac{1}{\alpha} (1 - \xi^2) \frac{m_0}{m^*[x(\xi)]}, \quad (12)$$

$$\nu(\xi) \equiv \frac{2\alpha}{1 - \xi^2} \frac{U[x(\xi)]}{E^*}, \quad (13)$$

$$\sigma(\xi) \equiv \frac{2\alpha}{1 - \xi^2}, \quad (14)$$

and dimensionless new, “reduced energy”, eigenvalue λ defined as

$$\lambda = \frac{E}{E^*}, \quad (15)$$

where E^* denotes a convenient energy scale

$$E^* \equiv \frac{\hbar^2}{m_0 x^{*2}} \equiv 1 \text{ eV}, \quad (16)$$

rendering the characteristic confinement length x^* entering the independent variable transformation (9) after the dimensionless scale factor α equal to $2.76043 \frac{0}{\text{\AA}}$, m_0 giving the electron rest mass.

For converting the Sturm – Liouville differential equation concerning the nanoheterointerface two-dimensional electron gas (2DEG) transformed wavefunction $\varphi(\xi)$ into a linearised

system of difference equations, we employ the numerical approximation

$$\frac{d}{d\xi} \left[\mu(\xi) \frac{d\phi(\xi)}{d\xi} \right] \rightarrow \frac{1}{k} \left[\mu_{i+\frac{1}{2}} \left(\frac{\phi_{i+1} - \phi_i}{k} \right) - \mu_{i-\frac{1}{2}} \left(\frac{\phi_i - \phi_{i-1}}{k} \right) \right], \quad (17)$$

in which the computational (nodal and interstitial, respectively) grid points ξ_n (whence $f_n \equiv f(\xi_n)$ with f standing for function ϕ , μ , v , and σ , as the case might be) are chosen as

$$\xi_i = -1 + ik \quad (i = 0, 1, 2, \dots, N+1),$$

$$\xi_{i \pm \frac{1}{2}} = \xi_i \pm \frac{k}{2} \quad (i = 1, 2, \dots, N+1), \quad (18)$$

for a uniform grid spacing

$$k = \frac{1 - (-1)}{N+1} = \frac{2}{N+1}, \quad (19)$$

and for which the adjoint boundary conditions become, after (5) & (12),

$$\phi_0 = \phi(\xi_0) = \phi(-1) = 0$$

&

$$\phi_{N+1} = \phi(\xi_{N+1}) = \phi(-1 + (N+1) \frac{2}{N+1}) = \phi(+1) = 0. \quad (20)$$

The Schrödinger equation eigenvalue problem is, thus, approximated by the system of difference equations

$$\{\alpha_i \phi_{i-1} + \beta_i \phi_i + \gamma_i \phi_{i+1} = -k^2 \Lambda \phi_i; i = 1, 2, \dots, N\} \quad (21)$$

or, equivalently, in tridiagonal matrix rows form,

$$\left\{ \sum_{j=1}^N \{[\alpha_i \delta_{i-1,j} + \beta_i \delta_{i,j} + \gamma_i \delta_{i+1,j}] \phi_j\} = -k^2 \Lambda \phi_i; i = 1, 2, \dots, N \right\}$$

$$-k^2 \Lambda \phi_i \quad ; \quad i = 1, 2, \dots, N \} \quad (22)$$

($\delta_{i,j}$ being the Kronecker delta), with the sets of coefficients $\alpha_i, \beta_i, \gamma_i$ defined as

$$\alpha_i \equiv \frac{\mu_{i-\frac{1}{2}}}{\sigma_i}, \gamma_i \equiv \frac{\mu_{i+\frac{1}{2}}}{\sigma_i}, \beta_i \equiv -(\alpha_i + \gamma_i + \frac{2}{\sigma_i} v_i); i = 1, 2, \dots, N, \quad (23)$$

and Λ denoting the approximation to the exact reduced energy eigenvalue λ (E_q , (15)), produced by the constructed numerical algorithm and expected to more closely converge to it with increasing number N of computational grid nodal points ξ_i utilised.

The treatment has, therefore, evolved into the matrix eigenvalue problem

$$\left\{ \sum_{j=1}^N \{\Lambda_{i,j} \phi_j\} = -k^2 \Lambda \phi_i; i = 1, 2, \dots, N \right\},$$

(24)

with the N -th order square tridiagonal matrix

$$\{(\Lambda_{i,j}; j = 1, 2, \dots, N); i = 1, 2, \dots, N\}$$

defined by

$$\Lambda_{i,j} \equiv \alpha_i \delta_{i-1,j} + \beta_i \delta_{i,j} + \gamma_i \delta_{i+1,j}.$$

(25)

Indeed; the opposite of the eigenvalues of matrix $\{\Lambda_{i,j}\}$ divided by k^2 give Λ , the approximations to the heterointerface wavefunction

exact reduced energy eigenvalues λ , thus computing (E_q , (15)) the allowed QW 2DEG subband energies $E = \lambda E^*$. Obviously, given that the general Sturm – Liouville system (10) may admit an infinite sequence of eigenvalues λ , the finite succession of N eigenvalues Λ for algorithmic matrix $\{\Lambda_{i,j}\}$ provides the numerical approximations to only the N lowest true reduced energy eigenvalues λ , a slightly lessening approximation sufficiency for the last higher order computed eigenvalues being algorithmically probable. On the other hand, the N determined, Sturm – Liouville eigenvectors $|\phi(\xi)\rangle$ conjugate to these numerical eigenvalues Λ unveil through transformation (9) the quantum mechanically allowed wavefunctions $\psi(x)$ for the 2DEG dwelling within the nanodevice heterointerface QW and underlying the crucial optoelectronic effects exhibited by the generic semiconductor nanostructure. In particular, such a determination of the nanoheterointerface 2DEG wavefunction may lead to the computation of its entailed penetration length into the nanodevice neighbouring energy barrier layer, thus facilitating the prediction of 2DEG mobility behaviour parameterised by the order of wavefunction excitation and, furthermore, the consideration of quantum mechanical tunnelling transmission probability for conductivity electrons escaping the heterointerface and travelling through the nanodevice – by virtue of a normal transport mechanism advantageously exploitable, especially at nanoelectronic cryogenic ambient temperatures.

In this manner, the partially localised conductivity electron eigenstates accommodated by the couple of communicating QWs in the model application under study correspond to the energy eigenvalues (measured within each QW from its energetic bottom upwards): $E(\mathbf{I}f>) = 32$ meV, $E(\mathbf{I}f'>) = 136$ meV – for the front QW fundamental and first excited bound state, respectively, – and $E(\mathbf{I}b>) = 14$ meV, $E(\mathbf{I}b'>) = 55$ meV, and $E(\mathbf{I}b''>) = 121$ meV – for the back QW fundamental, first excited, and second excited bound state, respectively.

Notably, against this predicted energy eigenvalue configuration, the fundamental back QW eigenstate $\mathbf{I}b>$ elevated by 14 meV over the back QW energetic bottom finds itself well aligned with the conjugate fundamental eigenstate $\mathbf{I}f>$ of the front QW raised above its QW energetic bottom by an amount corresponding to the inter – QW energetic bottom discrepancy plus, about, the former fundamental eigenstate $\mathbf{I}b>$ height over its local QW bottom.

In an analogous manner, the uppermost bound eigenstates of the two communicating QW, emerge aligned, as the difference in the height of each over its local QW bottom almost cancels the energetic height asymmetry of the two QW bottoms.

The ensuing calculations incorporate the determination of the effective dipole lengths associated with the intersubband transitions collaborating or antagonising with one another through the optoelectronic structure, an intersubband transition lifetime engineering thus emerging as a conformal mapping of the original

heterosturcture wavefunction-engineering attempted. The determined intersubband transition (ISBT) effective dipole lengths, furthermore, demonstrate the oscillator strengths supporting the different ISBT events, whereas the LASER action population inversion predicted leads to the device stimulated optical gain.

Our preliminary results (radiative transition time constant around 45 ns, corresponding to an ISBT dipole length $\langle b'' | z | b' \rangle$ around 1 nm), trace a LASER far mid – infrared emission OPRT functionality in the 65 meV / 15 THz range, with a stimulated optical gain Y sensitivity $\frac{\partial Y}{\partial I}$ to the pumping illumination power I around $11 \frac{\text{cm}^{-1}}{10^5 \text{ W/cm}^2}$.

References

- [1] J.J. Harris, R. Murray, and C. T. Foxon, *Semicond. Sci. Technol.* **8**, 31 (1993).
- [2] Shengs S. Li, M. Y. Chuang, and L. S. Yu, *Semicond. Sci. Technol.* **8**, S406. (1993).
- [3] L. V. Logansen, V. V. Malov, and J. M. Xu, *Semicond. Sci. Technol.* **8**, 568. (1993).
- [4] C. Juang, *Phys. Rev. B* **44**, 10706 (1991).
- [5] M. Ya. Asbel, *Phys. Rev. Lett.* **68**, 98 (1992).
- [6] G. J. Papadopoulos, *J. Phys. A.* **30**, 5497 (1997).

- [7] F. Capasso and A. Y. Cho, Surf. Sci. **299/300**, 878 (1994).
- [8] R. O. Grondin, W. Porod, J. Ho, D. K. Ferry, and G. J. Iafrate, Superlattices and Microstructures **1**, 183 (1985).
- [9] J. N. Churchill and F. E. Holmstrom, Phys. Lett A **85**, 453 (1981).
- [10] T. C. L. G. Sollner, W. D. Goodhue, P. E. Tannenwald, C. D. Parker, and D. D. Peck, Appl. Phys. Lett. **43**, 588 (1983).
- [11] N. Yokoyama, K. Imamura, T. Oshima, H. Nishi, S. Muto, K. Kondo, and S. Hiyamizu, Japan. J. Appl. Phys. **23**, L. 311 (1984).
- [12] J. Faist, F. Capasso, D. Sivco, D. Sirtori, A. L. Hutchinson S. N. G. Chu, and A. Y. Cho, Science **264**, 553 (1994).
- [13] J. Faist, F. Capasso, C. Sirtori, D. L. Sivco, A. L. Hutchinson, and A. Y. Cho, Electron. Lett. **32**, 560 (1996).
- [14] Jasprit Singh, *Semiconductor Optoelectronics* (McGraw – Hill, New York, 1995), Chap. 10.
- [15] G. H. Julien, O. Gauthier – Lafaye, P. Boucaud, S. Sauvage, J. – M. Lourtioz, V. Thierry – Mieg, and R. Phanel, *Intersubband Transitions in Quantum Wells: Physics and Devices* (Kluwer Academic Publishers, Boston, 1998), Chap. 1, Paper 2nd.
- [16] E. A. Anagnostakis, Phys. Stat. Sol. B **181**, K15 (1994).
- [17] G. Bastard, *Wave Mechanics Applied to Semiconductor Heterostructures* (Les Edition de Physique, Les Ulis Cedex – France, 1987), Chap. IV, VI.
- [18] Wen – Huei Chiou, Hsi – Jen Pan, Rang – Chau Liu, Chun – Yuan Chen, Chith – Kai Wang, Hung – Ming Chuang, and Wen – Chau Liu, Semicond. Sci. Technol **17**, 87 (2002).
- [19] M. Pessa, M. Guina, M. Dumitrescu, I. Hirvonen, M. Saarinen, L. Toikkanen, and N. Xiang, Semicond. Sci. Technol. **17**, R1 (2002).
- [20] J. M. Buldu, J. Trull, M. C. Torrent, J. Garcia – Ojalvo, and Claudio R. Mirasso, J. Opt. B: Quantum Semiclass. Opt. **4**, L1 (2002).
- [21] V. D. Kulakovskii, A. I. Tartakovskii, D. N. Krizhanovskii, N. A. Gippius, M. S. Skolnick, and J. S. Roberts, Nanotechnology **12**, 475 (2001).
- [22] E. A. Anagnostakis, J. Non-Cryst. Sol. **354**, 4233 (2008).